Hindawi
Journal of Nanomaterials
Volume 2021, Article ID 8871067, 9 pages
https://doi.org/10.1155/2021/8871067

Research Article

Synthesis, Characterization, and Photocatalytic Activity of g-C_3N_4/GaN-ZnO Composite

Nguyen Ha Trang,[1] Tran Thi Viet Ha,[1] Nguyen Minh Viet,[2] and Nguyen Minh Phuong[3]

[1]*Master's Program in Environmental Engineering, VNU Vietnam Japan University, Hanoi, Vietnam*
[2]*Key Laboratory of Advanced Material for Green Growth, Faculty of Chemistry, VNU University of Science, Hanoi, Vietnam*
[3]*Faculty of Chemistry, VNU Hanoi University of Science, Hanoi, Vietnam*

Correspondence should be addressed to Tran Thi Viet Ha; ttv.ha@vju.ac.vn

Received 17 September 2020; Revised 8 December 2020; Accepted 18 December 2020; Published 11 January 2021

Academic Editor: Nguyen Duc Cuong

Recently, photocatalysis process has shown great potential as a low-cost, environmentally friendly, and sustainable method for the water/wastewater treatment. Among that, g-C_3N_4 is one of the most promising photocatalyst and widely used for a variety of applications. In spite of some unique features such as strong reduction ability, active under visible light, nontoxic, and high stability, g-C_3N_4 photocatalytic capability under visible light is limited due to fast recombination rate of reactive charges. To deal with this issue, in this study, g-C_3N_4 is combined with GaN-ZnO for reducing the recombination rate of charge carriers and increasing the active sites. The g-C_3N_4/GaN-ZnO composite was characterized by several methods such as SEM, EDX, XRD, FT-IR, UV-Vis, and BET. It is also observed that the composite with outstanding features can work effectively under visible light; thus, it is likely to be widely applied in environment treatment, especially in antibiotic residue with more than 90% of tetracycline was decomposed after 3 hours.

1. Introduction

The development of the industry now depends strongly on fossil fuels which will be exhausted in the future. Therefore, renewable energy sources are considered as an excellent alternative fuel source with advantages such as being available and being clean energy, without affecting the environment when exploited. Among them, solar energy is a popular renewable energy source today. The use of sunlight-based environmental treatment techniques has become one of the most potential and environmentally friendly techniques. Another concern is the water pollution caused by textile dyes, organic contaminants, and especially antibiotic residues. Antibiotics are defined as compounds or substances that destroy or inhibit the growth of bacteria. They are compounds used in animal husbandry and to prevent or to treat infections for human health; sometimes, they are used as food preservatives. During wastewater treatment, the partial or incomplete metabolism and also the ineffective removal of antibiotics have created the way for antibiotics to enter the environment including water, sediment, and soil through discharging wastewater. These pollutants have a big impact on the life of species and environmental pollution. Therefore, the removal of these pollutants is necessary. In recent years, a sustainable treatment technology by using semiconductor photocatalytic has been introduced because of various potential such as a low-cost, environmental friendly, and suitable for water/wastewater industry. The advantage of this technology is to oxidize and remove the organic compounds and microorganisms in water. Varieties of techniques have been applied to degradation those organic contaminants including many kind of photocatalyst (g-C_3N_4, TiO_2, ZnO,...) which is known as one of the most promising technology [1–5].

In chemistry, photocatalysis is the acceleration of a photoreaction in the presence of a catalyst. Therefore, to achieve an ideal photocatalyst, semiconductor photocatalysts need to have a suitable band gap to utilize sufficient solar energy. The graphite carbon nitride (g-C_3N_4) is known as a metal-free polymer and a conjugative π structure material. This material

has many ideal properties, such as unique electric, optical, structural, and physicochemical properties; these properties already make g-C_3N_4-based materials become the ideal substance for catalytic and energy applications [6, 7]. This is a promising nonmetallic photocatalyst in the decomposition of pollutant organic matter in visible light and the analysis of water into hydrogen and oxygen. However, the using of these photocatalyts are still faced with some drawbacks, for example, the absorption of visible light is ineffective and the quick recombination of electron-hole [8]. To improve the photocatalytic performance of g-C_3N_4, various studies were conducted, including nonmetallic g-C_3N_4 doping. The doping of g-C_3N_4 by various elements such as B, C, P, and S [2, 9] has been successfully conducted; resulting in photocatalytic activity of the materials is greatly improved. The doping of g-C_3N_4 by nonmetallic elements has become a concerned topic of research, opening up a new field of research, preparing materials that have good photocatalytic effect under visible light which meet the practical requirements. In addition to enhance the photocatalytic activity by doping a nonmetal in the lattice, the addition of a metal or metal oxide on the surface of g-C_3N_4 has also been of interest recently. Among the metals, Ag is most concerned by the acceptable price and the ability to increase the activity of Ag nanoparticles. In this case, Ag acts both as a photosensitive agent to increase the ability to absorb visible light and to exhibit a surface plasmon effect [10]. The first SnO_2/g-C_3N_4 material was synthesized. The material consists of two components: g-C_3N_4 with a low specific surface area and SnO_2 nanoparticles with a large surface area. In this composite, SnO_2 nanoparticles dispersed well into g-C_3N_4. The interaction between the two components is very strong; this is confirmed by the band gap energy and network parameters. The synergistic interaction between the two components in the SnO_2/g-C_3N_4 material is due to the contribution of the π-π conjugate effect in g-C_3N_4, resulting in a significant improvement in the process of electron separation, creating from the interaction between the contact surfaces and the two components. On the other hand, nanometer-sized SnO_2 particles will increase the surface area of the material, thereby increasing photon efficiency. As a consequence, this material is an active photocatalytic, greatly increasing the decomposition of methyl orange (MO) under visible light irradiation. Optimum optical efficiency of up to >90% indicates that photocatalytic capacity is much higher than separate g-C_3N_4 and SnO_2 components [11]. Therefore, the modification of g-C_3N_4 to create new material with high photocatalytic efficiency is necessary.

Besides, GaN–ZnO solid solution is a homogeneous phase with a lattice structure, consisting of two GaN and ZnO members dissolved in solid-state. Normally, GaN is a solvent (with a higher content), while ZnO is a solute (with a lower content). In the following years, many of these scientists' works were also published in world-renowned journals on the separation of GaN-ZnO solid solutions. Since 2005, Domen [12] and colleagues have published a large number of works on GaN–ZnO solid solutions in world-famous magazines. Initially, the authors successfully synthesized the nano-sized RuO2-doped GaN–ZnO solid solution and used it as a photocatalyst material to effectively separate water in visible light. This is one of the first publications on analyzing water under visible light on an oxynitride photocatalyst as a GaN–ZnO solid solution doped with nano-sized RuO_2. In contrast to conventional nonoxide photocatalysts, such as CdS, the GaN–ZnO solid solution is a fairly stable material in the photocatalytic reaction [12]. In another study [3], the author showed nano-dispersed Rh-/-Cr_2O_3 particles (core/-shell) on GaN-ZnO as a catalyst for separation of pure water. Rh-Cr_2O_3-/-GaN-ZnO material has good photocatalytic ability in visible light area. Cr_2O_3 shell prevents the formation of H_2 and O_2 from water on Rh nanoparticles, allowing to destroy the chemical balance of the water separation reaction, whereby the photocatalytic reaction efficiency increases significantly. The core/shell structure enhances H_2 release compared to bare Rh nanoparticles. From these studies, it can be seen that the GaN–ZnO solid solution has a special and very attractive property in the field of photocatalyst. However, concentrated works are applied in the field of water separation to produce hydrogen. Although there are many advantages in photocatalysis, the solid solution of GaN–ZnO is still rarely applied in the treatment of toxic organic substances in water. Therefore, the task of the research is to study the modification of this material to treat organic matter polluting the water environment. This is not only of scientific significance but also of high practical value.

Recently, the combination of two types of materials is GaN–ZnO and graphite carbon nitrite g-C_3N_4 have been tested as photocatalysts [13]. Compared to other photocatalysts, GaN–ZnO and g-C_3N_4 have many advantages such as low band gap energy, activating in visible light, high surface area, and durable and can be synthesized in large quantities. In this paper, the g-C_3N_4/GaN-ZnO composite photocatalyst was synthesized by a simple method and has shown a significantly improved photocatalytic activity for tetracycline (TC) degradation.

2. Materials and Methods

2.1. Sample Preparation. All chemicals used in this work were analytical grade without further purification from Merck, Germany. Deionized (DI) water was used for the preparation of all required solutions.

The urea was calcinated to obtain g-C_3N_4. 5 g of urea was put in a crucible, sealed with aluminum foil (to prevent the sublimation of precursors as well as enhance the condensation to form g-C_3N_4), then place the crucible into the furnace. The samples were heated at temperatures of 550°C in 3 hours. Finally, the furnace was naturally cooled to room temperature. The obtained polymer g-C_3N_4 is a light yellow powder with different color intensity depending on the heat regime. The samples of synthetic g-C_3N_4 materials are denoted g-C_3N_4-T, where T is the heating temperature (550°C).

The GaN-ZnO powder sample was synthesized by adding 2 g of Ga_2O_3 and ZnO with molar ratio of 1 : 1 and 2 g of urea into an agate mortar and grind finely. The mixture was put into a porcelain boat, placed a ceramic boat in the middle of the quartz tube, and then put into a horizontal furnace. The mixture was calcinated in a stream of argon gas at

temperature of 900°C for 4 hours. The products are denoted GaN-ZnO-T, where T is the heating temperature (900°C).

The composite of g-C_3N_4/GaN-ZnO was synthesized by adding 0.15 g of GaN-ZnO synthesized sample above and 1.05 g of urea into an agate mortar and grind finely. Then, the mixture was put into a crucible, covered with layers of aluminum foil, and put into a furnace. The sample was calcinated at 550°C for 3 hours.

2.2. Characterization. X-ray diffractometer (XRD, Rigaku Miniflex II, Japan) is used to study the crystal structure, evaluate the crystallization level, and detect the strange crystal phase of the material. Fourier-transform infrared spectroscopy (FTIR) (Jasco 6100, Japan) is used for characterizing chemical bonds of materials. Energy dispersive X-ray (EDX) is to analyze the chemical elements of materials from Jeol EDS System. The image of sample surface is recorded by Scanning Electron Microscope (SEM) (Jeol JSM 7500FA, Japan), the signals used by a scanning electron microscope to produce an image result from interactions of the electron beam with atoms at various depths within the sample. Brunauer–Emmett–Teller (BET) (Jeol, Japan) is used to determine the surface area and the pore volume, and Diffuse Reflectance UV-vis Spectrum (UV-Vis-DRS) is to determine the band gap energy of materials.

2.3. Photocatalytic Activity Evaluation. Photocatalytic activities of g-C_3N_4/GaN-ZnO samples were evaluated by TC degradation in aqueous solution under visible light of 60 W lamp irradiation. TC stock solution (1000 mg/L) was prepared weekly using distilled deionized water and stored in dark at 4°C. The pH is adjusted by 1 mol/L of H_2SO_4 or NaOH, and C_0 and Ct are the concentrations of TC before and after photocatalytic reaction. The degradation of TC is considered through the decrease in its concentration versus irradiation time. The sample solutions were taken after 30 minutes. The TC solution obtained at times is diluted to the appropriate concentration, then measured based on the calibration curve to deduce the concentration of TC. They were analyzed using UV-Visible spectrophotometer with detection at 357 nm to take absorbance and from that take their concentration based on a calibration curve.

The removal efficiency of TC concentrations was calculated according to the differences between the initial and final concentrations. All the experiments were carried out at least three times, and the average values were calculated. The error between two experiments will not be greater than 10%.

3. Results and Discussions

3.1. Catalyst Characterization. The XRD patterns of g-C_3N_4, GaN-ZnO, and their synthesized composites are shown in Figure 1. The characteristic peaks appeared at 13.2° and 27.3° correspond to interlayer stacking of aromatic segments and tri-striazine units of pure g-C_3N_4 sample assigned to (100) and (002) planes [13, 14]. For GaN–ZnO material, the figure of XRD pattern shows that the peaks appear at 2θ = 32.39, 34.67, 36.42, 48.14, 57.74, 63.47, and 68.99 are typical diffraction patterns of GaN–ZnO solid solution,

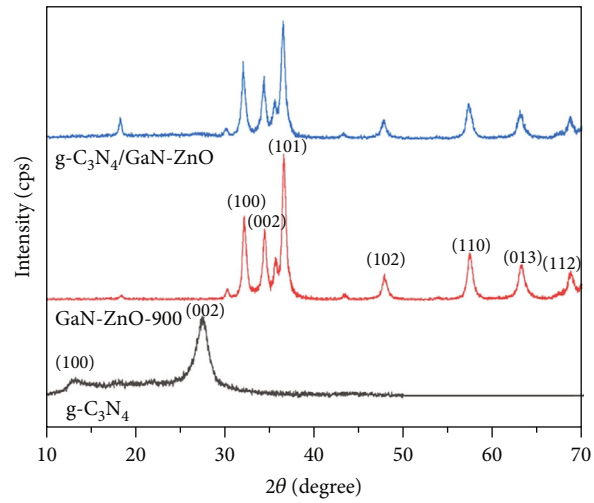

Figure 1: XRD patterns for gC_3N_4, GaN-ZnO, and gC_3N_4/GaN-ZnO composite.

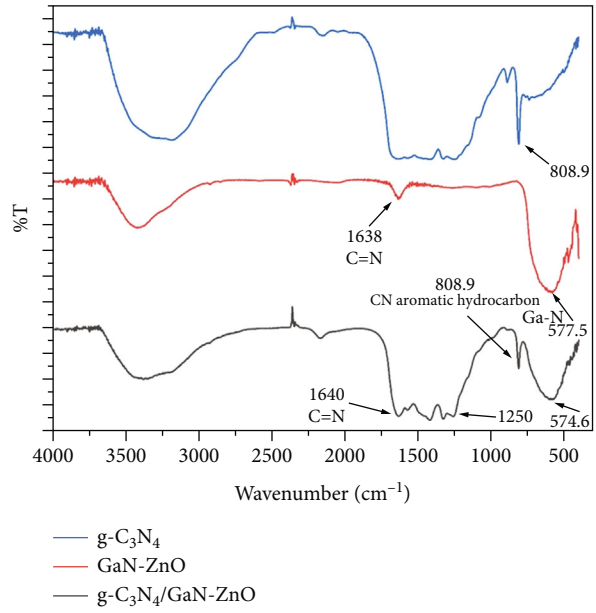

Figure 2: FT-IR spectrum for gC_3N_4, GaN-ZnO, and g-C_3N_4/GaN-ZnO composite.

corresponding to (100), (002), (101), (102), (110), (013), and (112) planes [13, 15]. Between peak of (002) and (101), there also appeared one extra strange peak thought to be of $ZnGa_2O_4$ spinene.

The g-C_3N_4/GaN-ZnO powder composites have diffraction peaks at 18.2, 32.3, 34.67, 36.42, 48.14, 57.74, 63.47, and 68.99°, which prove that the composites were successfully prepared.

IR spectra of the composites are showed in Figure 2. The IR spectrum appears almost all peaks of g-C_3N_4 and GaN-ZnO. At 808 cm^{-1} and some peaks in the range of 1250-1650 cm^{-1} are typical peaks for valence fluctuations of C-N bonds inside and outside the aromatic ring and the oscillation of the C=N bond. The broad absorption bands at

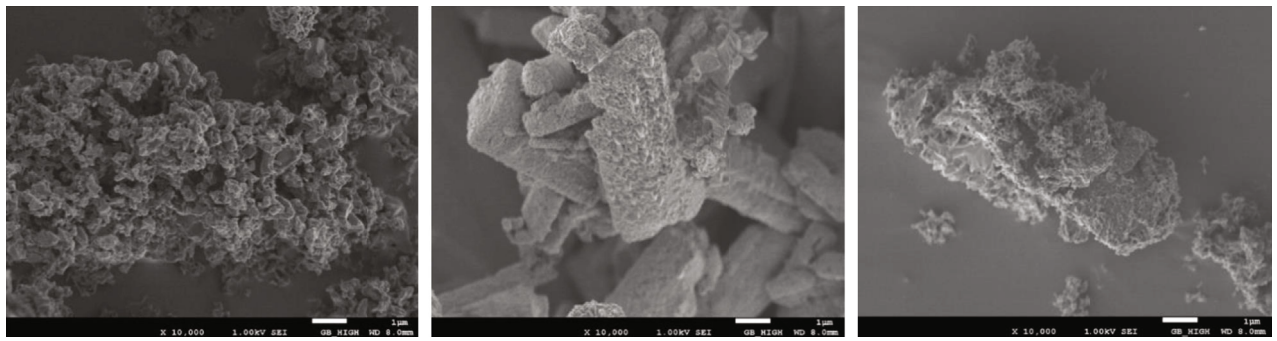

Figure 3: SEM image of g-C_3N_4, GaN-ZnO, and composite g-C_3N_4/GaN-ZnO.

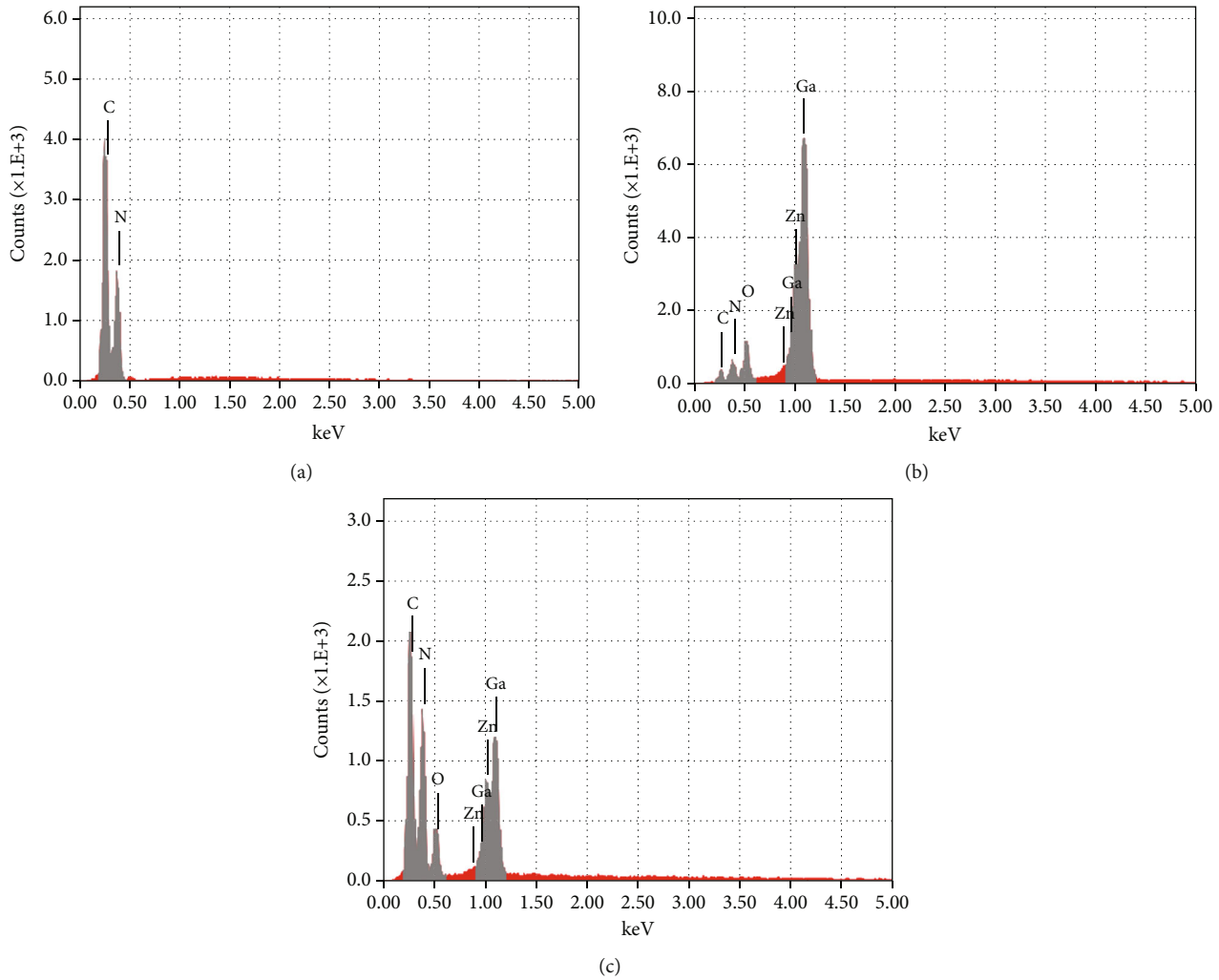

Figure 4: EDX spectra of g-C_3N_4 (a), GaN-ZnO (b), and g-C_3N_4/GaN-ZnO composite (c) materials.

3332.39–3186.8 cm^{-1} are oscillations of secondary and primary amines. These results are similar to previous reports [1, 11, 16]. When comparing the spectra of the composite and GaN-ZnO material, a wide absorption band at the number of waves above 3426 cm^{-1} and about 1638 cm^{-1} is the oscillation of -OH of physical absorbing water [15, 17]. The peak at the number of waves 494.6 cm^{-1} is the valence oscillation of the Zn–O bond [18]. In particular, the peak at 577 cm^{-1} of the solid solution featured for the bond of Ga-N was also discovered [17]. This proves that there are g-C_3N_4 and GaN-ZnO in the composite model.

Figure 3 shows the SEM images of GaN-ZnO and g-C_3N_4/GaN-ZnO material samples. The pure g-C_3N_4 catalyst sample is mainly in the form of low-porosity blocks. The GaN-ZnO samples had a clear shape of particles, while the g-C_3N_4/GaN-ZnO composite materials were blurred and no clear delineation between particles; the particles are covered by a thin film, which is thought to be of g-C_3N_4. The size of

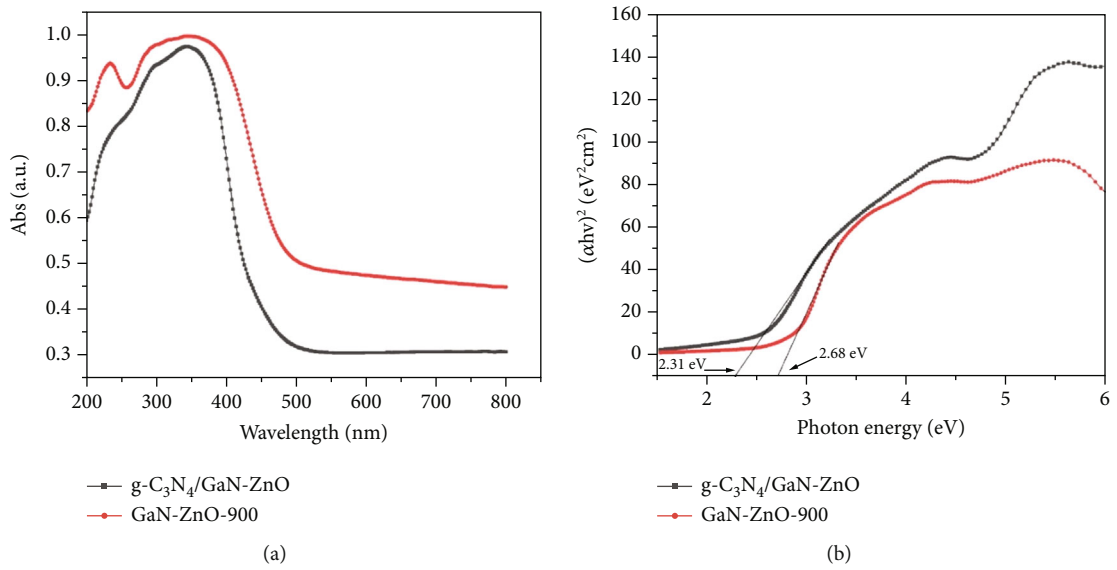

Figure 5: (a) UV-Vis-DRS spectra of GaN-ZnO and g-C_3N_4/GaN-ZnO (b). The energy band gap of GaN-ZnO and g-C_3N_4/GaN-ZnO.

the spherical particles is approximately 200 nm which is beneficial to enhance the photocatalytic efficiency of the synthesized material.

Elemental composition of g-C_3N_4/GaN-ZnO material samples characterized by EDX method is shown in Figure 4. This obtained result shows that the Ga, N, Zn, and O are detected with the percentage of mass of 30.65%, 6.00%, 7.99%, and 4.00%, respectively, while the element N content is still very low in the GaN-ZnO material sample. However, elemental element N significantly increased in the composite g-C_3N_4/GaN-ZnO material (21.64%). Figure 4(c) also indicates the appearance of C in the composite sample with the proportion of mass is 11.04%. This proves that there is an addition of element N into composite materials; the presence of element C in this spectrum further confirms the formation of composite materials from two components, g-C_3N_4 and GaN-ZnO. In particular, in this composite material sample, there is no presence of elements other than the constituent elements from the precursor materials. This further illustrates that the sample is not containing impurity, and the formation of composites is very good.

In addition, the optical properties of the material are determined by UV–Vis–DRS spectra; the results are shown in Figure 5. It can be noticed that the absorption peak and the light absorption edge of all materials are located in the visible light region (Vis region). From the results of UV-Vis-DRS spectroscopy, the band gap energy of GaN-ZnO and g-C_3N_4/GaN-ZnO composite was also determined in Figure 5(b). The band gap energy of GaN-ZnO and g-C_3N_4/GaN-ZnO composite was determined to be 2.68 eV and 2.31 eV. The band gap energy of g-C_3N_4 is 2.70 eV as reported in previous articles. Thus, the band gap energy of g-C_3N_4/GaN-ZnO composite is significantly lower than that of g-C_3N_4 and GaN-ZnO materials.

The BET surface areas and porous structures of g-C_3N_4, GaN-ZnO, and composite g-C_3N_4/GaN-ZnO are showed in Figure 6. In this figure, a type IV adsorption isotherm of the composite sample was showed with a hysteresis loop in the range ($P/P0$) of 0.6–1.0. The surface area and pore volume (Table 1) of g-C_3N_4 were 35.96 m^2/g and 0.114 cm^2/g,

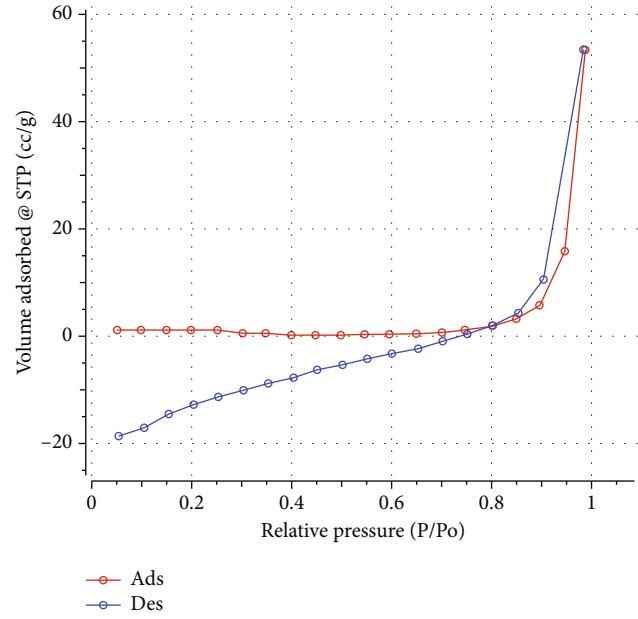

Figure 6: Nitrogen adsorption–desorption isotherm of composite g-C_3N_4/GaN-ZnO.

Table 1: Specific surface area, pore volume, and average pore radius.

Sample	Specific surface area (m^2/g)	Pore volume (cm^2/g)	Pore radius (nm)
g-C_3N_4	35.96	0.114	13.21
GaN-ZnO	2.787	0.014	5.840
g-C_3N_4/GaN-ZnO	9.515	0.075	13.21

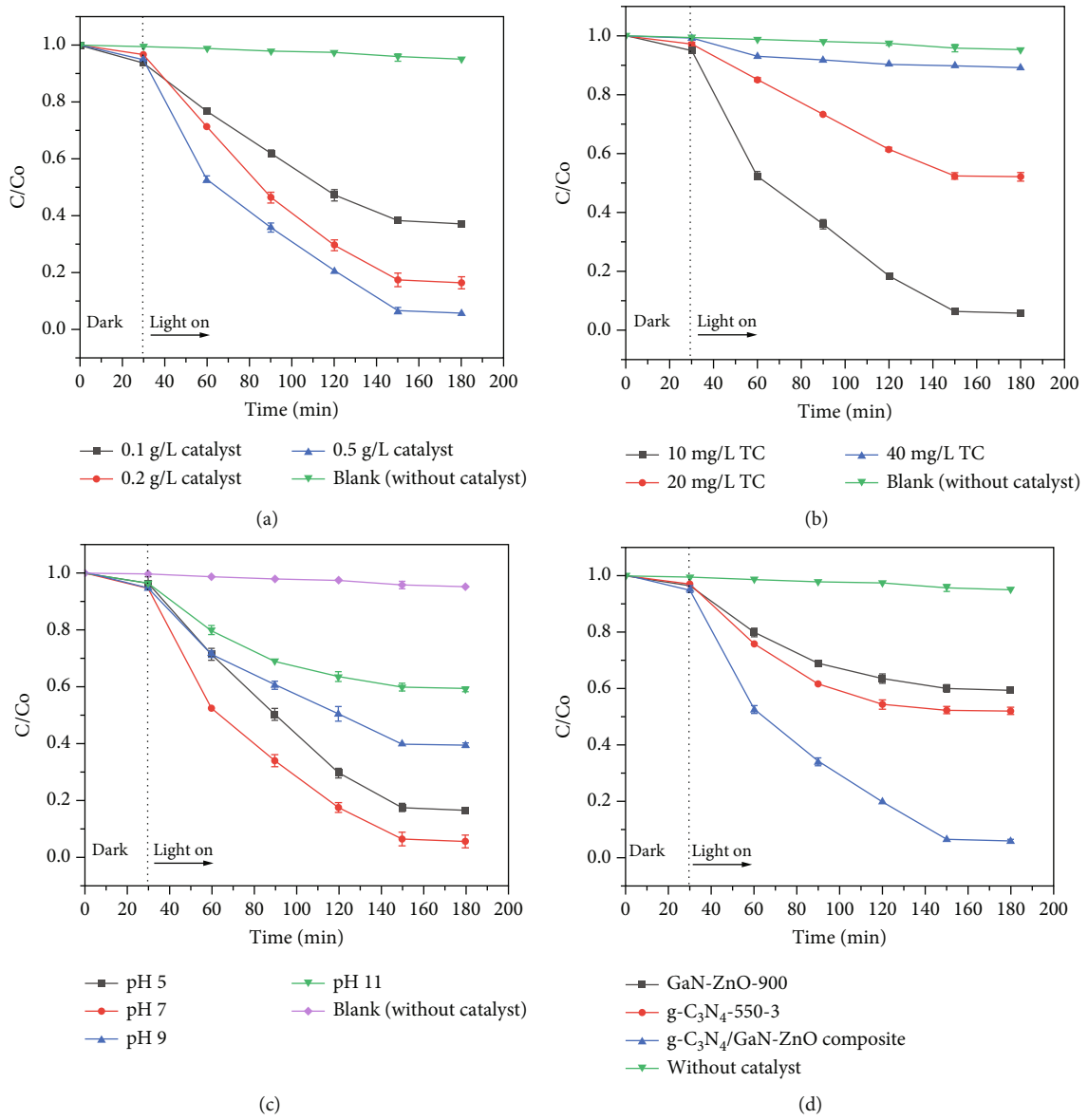

Figure 7: Degradation of TC under (a) various catalyst dosage, (b) various concentrations of TC, (c) initial pH, and (d) different materials.

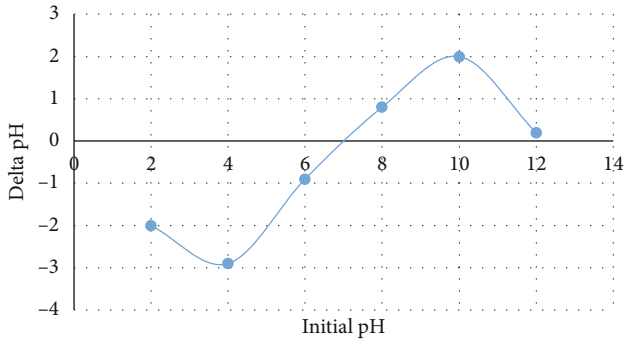

Figure 8: The plot of initial pH value versus delta pH value.

greater than GaN-ZnO and composite g-C_3N_4/GaN-ZnO (2.787 m^2/g, 0.014 cm^2/g and 9.515 m^2/g, and 0.075 cm^2/g, respectively). In the comparison of g-C_3N_4, the specific surface area of composite g-C_3N_4/GaN-ZnO was decreased, which is believed due to the presence of GaN-ZnO layers on the g-C_3N_4 surface. However, the surface area of composite g-C_3N_4/GaN-ZnO is not a main factor. Therefore, the improved photocatalytic performance is not influenced by the specific surface area. The increasing of photocatalytic activity of the composite materials is attributed to the more efficient separation of the photo-generated electron–hole pairs.

3.2. Photocatalytic Activity. In order to evaluate the effect of catalyst dosage, initial concentration, and initial pH on the removal efficiency, TC degradation experiments were conducted in various catalyst g-C_3N_4/GaN-ZnO weight (0.01, 0.02, and 0.05 g) and concentrations of TC (10, 20, and 40 mg/L) in the range of pH 5–11. Figure 7 shows the effect of catalyst dosage, initial concentration, and pH on the

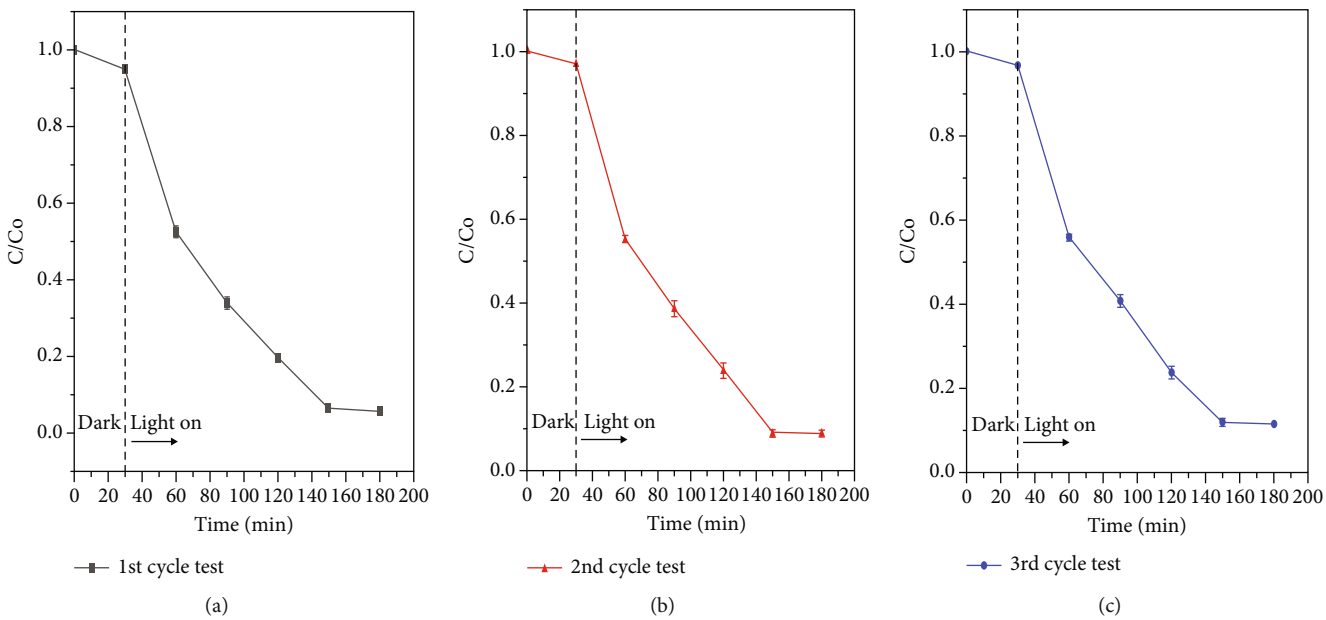

Figure 9: Cycling test for the degradation of TC by g-C_3N_4/GaN-ZnO composite.

removal efficiency of TC. After 30 min in the dark condition, only 5% of TC was absorbed on the surface of synthesized catalyst.

The results showed that the removal efficiency increased with the increasing of catalyst weight (Figure 7(a)). After 180 min of reaction time, 94.3% of TC was degraded by using appearance by using 0.05 g of catalyst. This result reflects the high removal efficiency at higher amount of catalyst. When the number of material particles increase, there are an increasing the number of photon and dye molecules absorbed. Therefore, the surface area of nanoparticles provides more active site to produce radicals for the reaction.

In Figure 7(b), the irradiation of TC solution with the initial concentrations of 10, 20, and 40 mg/L for 180 min leads to degradation of 94.5, 48.3, and 12.1% of TC. The degradation efficiency of TC decreased with the increasing initial concentration of the interest solution. These results can come from the reason that at higher concentrations, the concentration of intermediate products increases, and the hydroxyl radicals become the limiting reactant which leads to the decrease in degradation rate constant. Besides, when increasing the TC concentration, the TC molecules also increase which can cause the excessive adsorbed molecules into the surface of the material and the lack of contact between TC molecules and the photo-generated holes or hydroxyl radicals [19]. Therefore, the TC removal efficiency is decreased in case of increasing the initial concentration of pollutants.

One of the most important parameters in photocatalytic is the effect of pH. The change of the pH in a solution affects the charge properties of the material surface as well as regulates the ionization state of the catalyst surface. Therefore, pH influences the decomposition and adsorption capacity of organic compounds. The results in Figure 7(c) showed that the removal efficiency was most effective at pH of 7. At the TC concentration of 10 mg/L, irradiation of TC solution with the initial pH of 5, 7, 9, and 11 for 180 min leads to degradation of 67.2, 94.3, 60.4, and 40.7% of TC. These results are also explained by point zero charge of material (Pzc). The Pzc of the composite is determined at 6.9. To determine point of zero charge of g-C_3N_4/GaN-ZnO sample, the plot of delta pH value versus initial pH value was performed. The curve of this plot cut the horizontal axis at any pH which is the point zero charge of material. The obtained results were shown in Figure 8. If pH < Pzc, the positive charge of the g-C_3N_4 surface increases, and if pH > Pzc, the negative charge of the material surface increases. At acidic or alkaline, both the material surface and TC molecule are positive charge or negative charge. Therefore, the adsorption of TC on the surface of the material decreased, and the degradation will be more effective at neutral pH.

Figure 7(d) shows the TC degradation efficiency of g-C_3N_4, GaN-ZnO, and g-C_3N_4/GaN-ZnO materials. The synthesized g-C_3N_4/GaN-ZnO composite material showed highest degradation TC efficiency (95%) at pH = 7 (TC concentration = 10 mg/L) while the g-C_3N_4 and GaN-ZnO showed lower treatment rate with the removal efficiency of 38.1% and 20.5%, respectively. This result indicated that the synthesized g-C_3N_4/GaN-ZnO composite material can be utilized for tetracycline in the environment.

To assess the repeatability of the photocatalytic activity of composite sample, the cycling test was performed by doing several cycle experiments of TC degradation using g-C_3N_4/GaN-ZnO composite. The cycle time is 180 min. After collecting the composite samples from the previous step, the photocatalyst was filtered and dried at 105°C for 24 hours to use for the next cycle. As shown in Figure 9, nearly 90% of TC is still degraded by g-C_3N_4/GaN-ZnO composite after running 3 cycles, indicating quite good stability for photocatalytic degradation for TC.

The good repeatability of photocatalytic activity of g-C_3N_4/GaN-ZnO composite makes this material reusable many times when applied in practice.

The TC decomposition mechanism by synthesized g-C_3N_4/GaN-ZnO composite material is proposed in Figure 10. In this figure, after receiving visible light, the electron–hole separation occurs simultaneously on g-C_3N_4 and GaN–ZnO material; the electron moves to the conduction band (CB) and leaving the holes h + on the valence band (VB). In the conduction band, electrons from g-C_3N_4 will move to the GaN–ZnO of the composite, while in the valence band, the hole from GaN–ZnO will move to g-C_3N_4. This process significantly reduces electron-hole recombination occurring in composites. The reduction will occur in the conduction band of GaN-ZnO, and the oxidation will occur in the valence band of g-C_3N_4.

The following equations were used to determine conduction and valence band potentials of the synthesized samples.

$$\begin{aligned} E_{VB} &= \chi - E_e + 0.5E_g, \\ E_{CB} &= E_{VB} - E_g, \\ \chi &= \left[(\chi_{Ga}\chi_N)^{(1-x)} \cdot (\chi_{Zn}\chi_O)^x\right]^{1/2}, \end{aligned} \quad (1)$$

where χ is the semiconductor's electronegativity, the χ values for Ga, N, Zn, and O are 3.21, 7.27, 4.7, and 7.54 eV, respectively, and its values for GaN–ZnO were calculated as 5.03 eV. E_e is the free electron energy (4.5 eV) on hydrogen scale, E_g is the band gap energy, and E_{CB} and E_{VB} are the conduction and valence band potentials and have values -0.82 eV for CB potential and 1.86 eV for VB potential of GaN–ZnO. The E_{CB} and E_{VB} for g-C_3N_4 are -1.13 eV and 1.57 eV as reported in many previous researches.

$$\mathrm{g-C_3N_4/GaN-ZnO} + h\nu \rightarrow \mathrm{g-C_3N_4/GaN{-}ZnO}\left(e_{CB}^{-}h_{VB}^{+}\right)$$

$$\begin{aligned} &\mathrm{g-C_3N_4/GaN{-}ZnO}\left(e_{CB}^{-}h_{VB}^{+}\right) \rightarrow \mathrm{g{-}C_3N_4}\left(e_{CB}^{-}h_{VB}^{+}\right) \\ &\quad + \mathrm{GaN{-}ZnO}\left(e_{CB}^{-}h_{VB}^{+}\right) \end{aligned}$$

$$e_{CB}^{-} + O_2 \xrightarrow{h\nu} O_2^{\bullet -}$$

$$O_2^{\bullet -} + H^+ + 2e \rightarrow HO^{\bullet} + H^+$$

$$h_{VB}^{+} + H_2O \rightarrow HO^{\bullet} + OH^-$$

$$O_2^{\bullet -} + \mathrm{TC} \rightarrow \text{decomposition product}$$

$$HO^{\bullet} + \mathrm{TC} \rightarrow \text{decomposition product} \quad (2)$$

For g-C_3N_4/GaN-ZnO composites, g-C_3N_4 acts as a photosensitive agent, improving the ability to absorb visible light of composite materials. With this proposal mechanism, the photocatalytic activity of g-C_3N_4/GaN-ZnO composites was significantly improved compared to the separate semiconductors g-C_3N_4 and GaN-ZnO.

To further prove the possible photocatalytic mechanism, the PL spectra of g-C_3N_4/GaN-ZnO composite were obtained. As shown in Figure 11, the PL spectra of g-C_3N_4/GaN-ZnO composite were obtained with an excitation

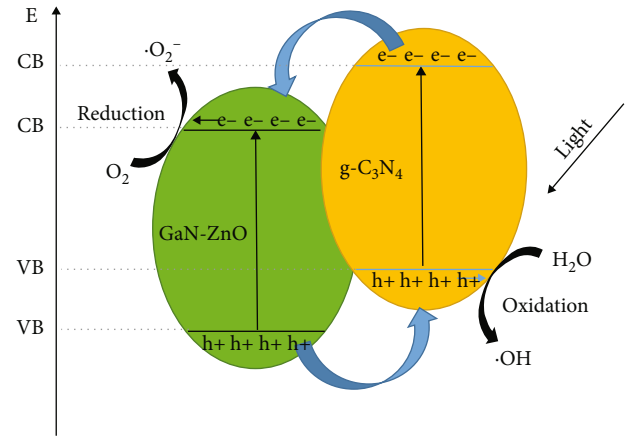

Figure 10: Mechanism of TC decomposition by g-C_3N_4/GaN-ZnO composite.

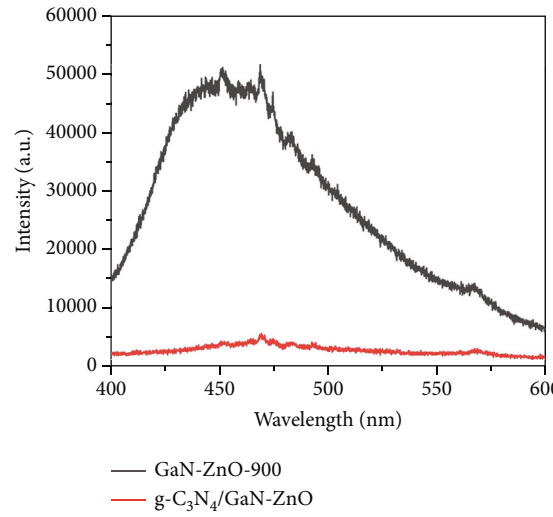

Figure 11: PL spectra of GaN-ZnO and g-C_3N_4/GaN-ZnO composite.

wavelength of 365 nm at room temperature. It can be seen from this figure that GaN–ZnO sample had much higher PL intensity than g-C_3N_4/GaN-ZnO composite which can be explained due to the higher recombination rate of charge carriers. In contrast, the intensity of g-C_3N_4/GaN-ZnO composite emission peak was decreased significantly, which illustrated that the recombination of the photo-generated carriers was reduced. The PL results have further confirmed the previous discussion on the photocatalytic mechanism and photocatalytic activity. The efficiently separated electrons and holes will greatly contribute to the photocatalytic reaction.

4. Conclusion

The novel g-C_3N_4/GaN-ZnO composites were successfully prepared by a simple calcination method. According to XRD pattern, IR spectrum, EDX, BET, UV-Vis-DRS, and SEM images, the presence of g-C_3N_4 and GaN-ZnO in the composite was observed. The resulting g-C_3N_4/GaN-ZnO composites showed an efficiency photocatalytic activity for

degradation of TC under visible light irradiation. Under the optimum experiment, the TC degradation of g-C_3N_4/GaN-ZnO is much higher than g-C_3N_4 and GaN-ZnO. 95% of TC was degraded by composite g-C_3N_4/GaN-ZnO in comparison with the degradation of 20-30% of TC by g-C_3N_4 and GaN–ZnO. Based on these findings, the g-C_3N_4/GaN-ZnO composites can be used as an alternative photocatalytic material for TC degradation in aqueous solutions or wastewater.

Data Availability

Data is available on request.

Conflicts of Interest

The authors declare that they have no conflicts of interest.

Acknowledgments

This work was supported by VNU Vietnam Japan University and Vietnam National Foundation for Science and Technology Development (NAFOSTED) under grant number 104.05-2019.336.

References

[1] L. Tian, X. Xian, X. Cui, H. Tang, and X. Yang, "Fabrication of modified g-C_3N_4 nanorod/Ag_3PO_4 nanocomposites for solar-driven photocatalytic oxygen evolution from water splitting," *Applied Surface Science*, vol. 430, pp. 301–308, 2018.

[2] M. Seredych, S. Łoś, D. A. Giannakoudakis, E. Rodríguez-Castellón, and T. J. Bandosz, "Photoactivity of g-C3N4/S-doped porous carbon composite: synergistic effect of composite formation," *ChemSusChem*, vol. 9, no. 8, pp. 795–799, 2016.

[3] T. Ohno, L. Bai, T. Hisatomi, K. Maeda, and K. Domen, "Photocatalytic water splitting using modified GaN: ZnO solid solution under visible light: long-time operation and regeneration of activity," *Journal of the American Chemical Society*, vol. 134, no. 19, pp. 8254–8259, 2012.

[4] H. Hao and J. Zhang, "The study of Iron (III) and nitrogen co-doped mesoporous TiO_2 photocatalysts: synthesis, characterization and activity," *Microporous and Mesoporous Materials*, vol. 121, no. 1-3, pp. 52–57, 2009.

[5] M. Boroski, A. C. Rodrigues, J. C. Garcia, L. C. Sampaio, J. Nozaki, and N. Hioka, "Combined electrocoagulation and TiO_2 photoassisted treatment applied to wastewater effluents from pharmaceutical and cosmetic industries," *Journal of Hazardous Materials*, vol. 162, no. 1, pp. 448–454, 2009.

[6] Y. Tachibana, L. Vayssieres, and J. R. Durrant, "Artificial photosynthesis for solar water-splitting," *Nature Photonics*, vol. 6, no. 8, pp. 511–518, 2012.

[7] H. Tong, S. Ouyang, Y. Bi, N. Umezawa, M. Oshikiri, and J. Ye, "Nano-photocatalytic materials: possibilities and challenges," *Advanced Materials*, vol. 24, no. 2, pp. 229–251, 2012.

[8] J. Wen, J. Xie, X. Chen, and X. Li, "A review on g-C_3N_4-based photocatalysts," *Applied Surface Science*, vol. 391, pp. 72–123, 2017.

[9] L. Chen, X. Zhou, B. Jin et al., "Heterojunctions in g-C_3N_4/B-TiO_2 nanosheets with exposed {001} plane and enhanced visible-light photocatalytic activities," *International Journal of Hydrogen Energy*, vol. 41, no. 18, pp. 7292–7300, 2016.

[10] Y. Chen, W. Huang, D. He, Y. Situ, and H. Huang, "Construction of heterostructured g-C3N4/Ag/TiO2Microspheres with enhanced photocatalysis performance under visible-light irradiation," *ACS Applied Materials & Interfaces*, vol. 6, no. 16, pp. 14405–14414, 2014.

[11] Y. Zang, L. Li, X. Li, R. Lin, and G. Li, "Synergistic collaboration of _g_ -C_3N_4/SnO_2 composites for enhanced visible-light photocatalytic activity," *Chemical Engineering Journal*, vol. 246, pp. 277–286, 2014.

[12] X. Lu, A. Bandara, M. Katayama, A. Yamakata, J. Kubota, and K. Domen, "Infrared spectroscopic study of the potential change at cocatalyst particles on oxynitride photocatalysts for water splitting by visible light irradiation," *The Journal of Physical Chemistry C*, vol. 115, no. 48, pp. 23902–23907, 2011.

[13] M. Yang, Q. Huang, and X. Jin, "ZnGaNO solid solution-C_3N_4 composite for improved visible light photocatalytic performance," *Materials Science and Engineering: B*, vol. 177, no. 8, pp. 600–605, 2012.

[14] X. Li, J. Zhang, L. Shen et al., "Preparation and characterization of graphitic carbon nitride through pyrolysis of melamine," *Applied Physics A*, vol. 94, no. 2, pp. 387–392, 2009.

[15] K. Maeda and K. Domen, "Solid solution of GaN and ZnO as a stable photocatalyst for overall water splitting under visible light," *Chemistry of Materials*, vol. 22, no. 3, pp. 612–623, 2010.

[16] Z. Yong, J. Ren, H. Hu et al., "Synthesis, characterization, and photocatalytic activity of g-C3N4/KTaO3 composites under visible light irradiation," *Journal of Nanomaterials*, vol. 2015, 7 pages, 2015.

[17] V. N. Bessolov, Y. V. Zhilyaev, E. V. Konenkova, V. A. Fedirko, and D. R. T. Zahn, "Raman and infrared spectroscopy of GaN nanocrystals grown by chloride-hydride vapor-phase epitaxy on oxidized silicon," *Semiconductors*, vol. 37, no. 8, pp. 940–943, 2003.

[18] A. Sharma and S. Pallavi, "Synthesis and characterization of NiO-ZnO nano composite," *Nano Vision*, vol. 1, no. 115, pp. 112–115, 2012.

[19] G. H. Safari, M. Hoseini, M. Seyedsalehi, H. Kamani, J. Jaafari, and A. H. Mahvi, "Photocatalytic degradation of tetracycline using nanosized titanium dioxide in aqueous solution," *International journal of Environmental Science and Technology*, vol. 12, no. 2, pp. 603–616, 2014.